

carbon. Some of the diamonds are single crystals; most of them are polycrystalline. Electron diffraction of the latter show a ring pattern, which can be indexed by (111), (220), (113), (400) according to the space group Fd-3m of diamond. A weak preferred orientation of the very small crystallites is indicated by maxima in the ring pattern. Beside the diamond inclusions there are other inclusions, of similar or smaller grain size, like corundum, aragonite or orthopyroxene.

The first observation of diamonds in melt inclusions in Hawaiian lava might give insights both into the formation of diamonds and the geochemical processes operating in the mantle beneath the Hawaiian Island chain.

## V22A-1213 1330h POSTER

### Cooling Rate and Isothermal Crystallization Effects on Melt Inclusion Formation in MORB High-An Feldspar and High-Fo Olivine

Edward J Kohut<sup>1</sup> (541-737-8586; kohute@geo.orst.edu)

Roger L Nielsen<sup>1</sup> (541-737-3023; nielsenr@geo.orst.edu)

<sup>1</sup>Dept. of Geosciences, Oregon State University, 104 Wilkinson Hall, Corvallis, OR 97330, United States

The uncertainty regarding the nature of entrapment mechanisms is an important issue in melt inclusion studies. One example of this problem involves melt inclusions within high-An feldspar and high-Fo olivine phenocrysts that are commonly present in MORB lavas. Such inclusions are valuable potential sources of information on the diversity of MORB parent magmas, and in many cases their major element compositions are consistent with a parental relationship with the host. However, some of the inclusions in N-MORB phenocrysts are anomalously depleted in some minor and trace elements, and it is not clear whether this diversity can be attributed in any way to the entrapment process.

We have addressed this problem through a series of experiments using anorthite/ferroite saturated anhydrous mafic liquids cooled to 1230° and 1210° C from 1300° C. The liquids were cooled at rates of 1°, 5°, and 10°/min. followed by 0-24 hours isothermal periods. We observed that primary melt inclusion formation is related to crystal morphology, which is a function of the degree of undercooling, cooling rate, and length of the isothermal period. Hopper and skeletal morphologies form during the cooling period, and planar overgrowth of these textures during the isothermal period forms the majority of inclusions. Our results indicate that 1° and 5°/min. cooling rates are the most favorable for hopper and skeletal crystal morphologies, and the greatest frequency of inclusions occurs with 5°/min. (for feldspar) and 1°/min (for olivine) cooling, followed by 6 hours isothermal time. With increasing isothermal time past 6 hours, the frequency of inclusions decreases and the size of the crystals increases. This may indicate that Ostwald ripening plays a role in controlling inclusion frequency during longer isothermal periods. The length of the isothermal period required for the formation of most inclusions precludes the trapping of a boundary layer or diffusional profile, and all inclusions in olivine and plagioclase formed during the isothermal period have compositions identical to the surrounding glass. Significantly, no difference between K<sub>2</sub>O contents of host glass and melt inclusions was observed and there is no evidence for the formation of low-Ti inclusions.

We propose that primary inclusion formation may result from a moderate amount of undercooling followed by a short isothermal period and subsequent quenching. Such circumstances could occur in nature when a partial melt rises in a conduit into cooler crust and stagnates at shallow levels for a short period before an eruption.

## V22A-1214 1330h POSTER

### Ca-rich Plagioclase in Island Arc Tholeiite: Approaches from Hydrus Melting Experiments and Melt Inclusion Study

Morihiisa Hamada<sup>1</sup> (+81-3-5841-5829; morihiisa@magma.eri.u-tokyo.ac.jp)

Toshitsugu Fujii<sup>1</sup> (+81-5841-5751; fujii@eri.u-tokyo.ac.jp)

<sup>1</sup>Earthquake Research Institute, University of Tokyo, 1-1-1 Yayoi, Bunkyo-ku, Tokyo 113-0032, Japan

Ca-rich plagioclase phenocrysts (~An90) are often observed in island arc tholeiite. As the Ca/Na partitioning between plagioclase and dry basalt magma do not allow the crystallization of such Ca-rich plagioclase from bulk composition, they are considered to have crystallized from hydrous and/or primitive Ca-rich magma. However, their crystallizing conditions are

not constrained well, partly because the previous melting experiments at hydrous condition do not cover the compositions of the low-K island arc tholeiites. For this reason, the hydrous melting experiments on low-K island arc tholeiite from the Izu-Oshima volcano, Japan, were performed to understand the effect of water on the phase relation and the origin of the Ca-rich plagioclase.

Two kinds of relatively undifferentiated basalt with different Ca/Na ratio were prepared as starting materials: aphyric MA44 and porphyritic MA43. The experiments were performed under 2.5 kbar and Ni-NiO buffer using an internally heated pressure vessel. Water content was varied from 0 through 6 wt.%.

The plagioclase was consistently the first liquidus phase for the porphyritic sample MA43 for any water content, but augite replaced plagioclase as the first liquidus phase with increasing water for the aphyric MA44. The Ca/Na partitioning coefficient between plagioclase and melt increases with increasing water content in the melt and no temperature effect was detected and this was confirmed by the calculation of the MELTS program. The obtained results suggest that more than 3 wt.% of water in the melt is necessary to crystallize plagioclase of ~An90 from the bulk composition.

In order to confirm this estimation, the chemical compositions and the water content of the melt inclusions contained in the natural Ca-rich plagioclase phenocrysts from the Izu-Oshima volcano were examined. The melt inclusions show a wide range of composition suggesting the inclusions were enclosed at various stage of differentiation although the host plagioclase composition is relatively homogeneous. The water contents of the melt inclusions were only 1 wt.% at maximum. The compositional variation within melt inclusion overlaps with the differentiation trend obtained from the analysis of bulk rock chemistry of the Izu-Oshima volcano. The chemical composition and water content in the melt inclusions suggest that the origin of Ca-rich plagioclase can be explained neither by the presence of the extremely Ca-rich melt nor the equilibrium crystallization from the hydrous melt of more than 3 wt.% H<sub>2</sub>O.

## V22A-1215 1330h POSTER

### High-Ca Melt Inclusions in Primitive Shoshonites: Magma-Wall Rock Interactions?

Roman A Leslie<sup>1</sup> (61-3-62262376; rleslie@postoffice.utas.edu.au)

Leonid V Danyushevsky<sup>1</sup> (61-3-62262469; l.dan@utas.edu.au)

<sup>1</sup>School of Earth Sciences and CODES SRC, University of Tasmania, GPO Box 252-79, Hobart, TAS 7001, Australia

Pliocene absarokites from Tavua and Astrolabe Group volcanoes (Fiji) contain olivine phenocrysts Fo 93-72. Primitive olivines (>Fo 85) show a significant range in CaO content (0.1-0.47 wt% CaO), with high-Ca olivine (>0.35 wt% CaO) being most abundant. Melt inclusions (MI) hosted by high-CaO olivine are large and numerous. On the other hand, low-CaO primitive olivines are either devoid of MI, or MI tend to be smaller and comparatively less abundant. Prior to analysis, MI have been reheated to 1160-1325 °C for 3-5 min. and quenched to glass. MI hosted by evolved olivine (<Fo85) have compositions that match evolved rocks of the suites. In contrast, primitive high-CaO olivine hosts contain MI with very high CaO (up to 19 wt%), low SiO<sub>2</sub> and Al<sub>2</sub>O<sub>3</sub>, resulting in extreme CaO/Al<sub>2</sub>O<sub>3</sub> ratios (up to 1.95). The less abundant and comparatively smaller MI, hosted by primitive medium-CaO olivine (CaO 0.25-0.35 wt%) have compositions representative of primitive shoshonitic melts. They have higher SiO<sub>2</sub> and 'normal' CaO (10-14wt%) and Al<sub>2</sub>O<sub>3</sub> (13-17wt%), resulting in CaO/Al<sub>2</sub>O<sub>3</sub><1. Low-CaO olivines (<0.25 wt%) contain rare low-CaO, low-SiO<sub>2</sub> MI with high Na<sub>2</sub>O, K<sub>2</sub>O and TiO<sub>2</sub> contents. Occurrence of large and numerous MI in high-CaO olivines reflects rapid magma cooling and olivine growth. An environment where this can occur is at margins of a hot magma body where it interacts with colder wallrocks. The high-CaO MI in these olivines may then represent hybrid melts formed during localised assimilation. Less abundant, smaller primitive MI with "normal" compositions are likely trapped within the slow-cooling bulk of the magma, and are under represented due to a sampling bias phenomenon whereby hybrid melts are preferentially trapped during fast crystallisation.

## V22A-1216 1330h POSTER

### Source of Detrital Chrome Rich spinels with melt inclusions from the Cretaceous greywackes of the eastern Tethyan Himalayas: hot spot volcanics, not ophiolites

Bin Zhu<sup>1</sup> (zhub@atmos.albany.edu)

William S.F. Kidd<sup>1</sup> (wkidd@atmos.albany.edu)

David B. Rowley<sup>2</sup> (rowley@plates.uchicago.edu)

John W. Delano<sup>1</sup> (jdelano@atmos.albany.edu)

Brian S. Currie<sup>3</sup> (curriebs@muohio.edu)

<sup>1</sup>Earth and Atmospheric Sciences, University at Albany, 1400 Washington Avenue, Albany, NY 12222, United States

<sup>2</sup>Geophysical Sciences, University of Chicago, 5734 S. Ellis Avenue, Chicago, IL 60637, United States

<sup>3</sup>Department of Geology, Miami University, 114 Shideler Hall, Oxford, OH 45056, United States

Chrome rich spinel is a detrital component in turbidites from the well-exposed, mid-late Cretaceous Tianba Fylsch sequence in the Nieru Valley, southern Tibet. Microprobe results indicate that the spinels have a well-developed Fe-Ti trend, and have Cr/(Cr+Al) 0.4-0.65, Mg/(Mg+Fe<sup>2+</sup>) 0.3-0.9, and TiO<sub>2</sub> >1 wt.%. The compositional range of these detrital spinels closely matches that of spinels from intraplate basalts, and is very similar to spinel inclusions in olivine from Hawaii and Disko Island. In addition, 5% spinels contain melt inclusions of 0.005-0.06 mm diameter, glassy or partly crystallized. To homogenize the crystallized melt inclusions for subsequent analysis by electron microprobe, spinels were heated at 1250 °C for 96 hours at controlled oxygen fugacity (FMQ) and quenched. Compositions of homogenized melt inclusions are (in wt.%): SiO<sub>2</sub> (42-55), TiO<sub>2</sub> (1.5-3), Al<sub>2</sub>O<sub>3</sub> (11.5-15), MgO (9-13), CaO (6-12), Na<sub>2</sub>O (2-2.5), K<sub>2</sub>O (0.5-1.1), and CaO/Al<sub>2</sub>O<sub>3</sub> (0.7-1.0), which indicates an alkali basalt affinity. The compositions of melt inclusions correlate well with the compositions of host spinels, and both show a possible cocrystallization of olivine and spinel in the parental magma. Based on palaeo-tectonic reconstruction, presence of mid-late Cretaceous fossils in the strata, and the chemical compositions of spinels and associated melt inclusions, we conclude that volcanics of the Rajmahal, which are associated spatially and temporally with Kerguelen hotspot activity on India about 117 Ma ago, were the source for these Cr-rich spinels. Although the Tianba Fylsch looks in the field like a typical collisional product, and the presence of Cr-rich spinels might suggest an ophiolitic source and a Cretaceous ophiolite-obduction on the northern Indian continental margin, our detailed work shows clearly that the Tianba Fylsch is neither ophiolite-derived, nor related to the start of the India-Asia collision.

## V22A-1217 1330h POSTER

### Melt Inclusion Volatile Contents, Pressures of Crystallization for Hawaiian Picrites, and the Problem of Shrinkage Bubbles

Pablo Cervantes<sup>1</sup> (p0c2620@geo.tamu.edu)

Vadim Kamenetsky<sup>2</sup> (Dima.Kamenetsky@utas.edu.au)

Paul Wallace<sup>3</sup> (pwallace@darkwing.uoregon.edu)

<sup>1</sup>Texas A&M University, Department of Geology and Geophysics, College Station, TX 77845, United States

<sup>2</sup>University of Tasmania, Centre for Ore Deposit Research, Hobart 7001, Australia

<sup>3</sup>University of Oregon, Department of Geological Sciences, Eugene, OR 97403, United States

The H<sub>2</sub>O and CO<sub>2</sub> contents of melt inclusions can potentially be used to infer pressures of crystallization and inclusion entrapment because the solubility of mixed H<sub>2</sub>O-CO<sub>2</sub> vapor has been determined experimentally for basaltic and rhyolitic melts. However, melt inclusions commonly develop shrinkage bubbles caused by the greater thermal contraction of the melt compared with the host mineral during post-entrapment cooling. Because the solubility of CO<sub>2</sub> in silicate melts is much less than that of H<sub>2</sub>O, resulting in relatively high vapor-melt partition coefficients for CO<sub>2</sub>, formation of a shrinkage bubble can strongly deplete the coexisting melt of dissolved CO<sub>2</sub> that was present at the time of entrapment. To investigate the loss of CO<sub>2</sub> into shrinkage bubbles, we have experimentally reheated large melt inclusions in olivines from a Mauna Loa picrite in order to redissolve the vapor in the bubble. The olivines were sampled from Puu Wahi, a scoria cone situated at ~3000 m elevation on the NE rift zone of Mauna Loa. The olivines (Foggs) come from reticulite scoria and so were naturally quenched to glass during eruption, but all inclusions contain shrinkage bubbles < 3 vol% of the inclusion. Reheating to 1400°C remobilized the shrinkage bubble into the melt, but even with rapid quenching a small vapor bubble formed during quench. CO<sub>2</sub> contents measured by FTIR spectroscopy and recalculated for melt in equilibrium with the olivine host are 300-600 ppm (n=11) for reheated inclusions, much higher than the CO<sub>2</sub> contents of the naturally quenched inclusions (60-180 ppm; n=8), which all contain shrinkage bubbles. Dissolved H<sub>2</sub>O contents of the melt inclusions are very uniform (0.36 ± 0.05 wt%). Pressures of inclusion entrapment

basaltic scoria samples from Guguan, Pagan and Agrigan islands of the Mariana arc. The MIs studied are olivine-hosted (Fo 68-82), 50-300 m, clear brown glass with no visible evidence of devitrification. We have analyzed these MIs for H<sub>2</sub>O and CO<sub>2</sub> by FTIR, major elements by EMP and trace elements by laser ablation ICP-MS. The MIs range in water content from 1-4 wt.%, but MIs with detectable CO<sub>2</sub> indicate a tighter range of H<sub>2</sub>O concentrations in undegassed inclusions from 2.5-4 wt.% and averaging 3 wt.% H<sub>2</sub>O. The MIs are broadly similar in both major and trace elements to lavas from the same islands, but these new data extend the range of trace element compositions observed in Mariana arc lavas. We have analyzed MIs from Agrigan with trace element systematics nearly identical in Ba/La and La/Sm to that of bulk subducting sediment in the Marianas, and from Guguan with a composition very close to the inferred slab-derived fluid composition. One Guguan inclusion is of particular interest. It has 3.5 wt.% H<sub>2</sub>O with an NMORB REE pattern (La/Sm=0.76), high Ba/La (70) and very high U/Th (1.1). It also has high Pb/U (25) demonstrating a preference for Pb over U in slab-derived fluids. The composition of this inclusion also plots near the y-intercept (zero sediment flux) on global arc-sediment flux correlation diagrams, confirming that it represents close to an average global sediment-free slab fluid composition. Compositions this extreme have never been measured in Mariana arc lavas before. On the other hand, this fluid-rich arc melt has a very different composition from a comparable melt calculated using the H<sub>2</sub>O-rich component of Stolper & Newman (1994) for the Mariana back-arc, which has lower Ba/La (11), U/Th (0.4) and Pb/U (4.2). This contrast in arc and back-arc fluids is suggestive of two potential processes. A similar slab-derived fluid may be added to variably depleted mantle, less depleted in the back-arc and more depleted beneath the arc. Alternatively, the slab may undergo progressive dehydration, where sub-arc dehydration removes fluid-mobile elements and depletes the slab of such elements before further dehydration in the back-arc.

## V21C-11 1120h

### Water Abundance in Arc Magmas: Olivine Melt Inclusions From Central America

Kurt Roggensack<sup>1</sup> (480-759-3886;  
kurt.roggensack@asu.edu)

Richard L. Hervig<sup>1,2</sup> (richard.hervig@asu.edu)

<sup>1</sup>Department of Geological Sciences, Arizona State University, Tempe, AZ 85287-1404, United States

<sup>2</sup>Center for Solid State Science, Arizona State University, Tempe, AZ 85287-1704, United States

Water and CO<sub>2</sub> variation in arc magmas has been investigated using olivine melt inclusions from nine scoria and ash deposits in Central America. Samples from Nejapa and Granada regions of Nicaragua are among the most primitive (bulk MgO 6.9 to 8.8 wt.%), have moderate Ba/La ratios (30 to 60) and contain olivine phenocrysts of composition Fo<sub>91-86</sub>. Melt inclusions within these deposits are characterized by low to moderate water and high CO<sub>2</sub> (2 to 3.5 wt.% and 1,000 to 2,500 ppm, respectively; determined by FTIR). Other Nicaraguan (including Momotombo, Cerro Negro, Telica) and Guatemalan (Fuego) samples are more evolved (bulk MgO 3.4 to 6.4 wt.%), have moderate to high Ba/La ratios (52 to 116) and contain olivine phenocrysts of composition Fo<sub>78-82</sub>. Melt inclusions are characterized by high water contents (generally 3.5 to 4 wt.%) and CO<sub>2</sub> of 1,200 ppm or less. Many samples (including primitive Nejapa and Granada) show evidence of heterogeneity. For example, high-TiO<sub>2</sub> inclusions are sometimes found in low-TiO<sub>2</sub> magmas and vice versa, or low-Ba and Ba inclusions are found in units where high-Ba and Ba inclusions predominate. Also, some individual eruptive units display heterogeneity in water abundance. For instance, some define steep CO<sub>2</sub>-degassing trends at nearly constant water while others show significant H<sub>2</sub>O variation (1 to 1.5 wt.%; ~30% relative) at elevated CO<sub>2</sub> that cannot be explained by degassing. Instead, the heterogeneity in water and major and trace elements suggests that individual eruptive units are comprised of variably admixed magma batches. In the Nejapa and Granada area, where the arc signature is less pronounced, there is an apparent positive correlation between water abundance (average melt inclusion) and bulk-determined (ICP-MS) incompatible elements (K, Rb, Ba, Sr, Pb, U) with low-TiO<sub>2</sub> magmas having higher water abundance than high-TiO<sub>2</sub> magmas. In contrast, volcanic units with stronger arc signatures show no correlation between water and trace elements. The latter observation may be caused by multiple additions of slab-derived material to the magma source region.

## V21C-12 1135h

### Pre-eruptive Volatile Concentrations in Rhyodacitic Melt Inclusions From Mt. Mazama: Implications for Eruption Triggering

Charles W. Mandeville<sup>1</sup> (212-769-5380;  
cmandy@amnh.org)

James D. Webster<sup>1</sup> (212-769-5401; jdweb@amnh.org)

Charles R. Bacon<sup>2</sup>

<sup>1</sup>American Museum of Natural History, Central Park West at 79th St, New York, NY 10024, United States

<sup>2</sup>U.S. Geological Survey, 345 Middlefield Rd., Menlo Park, CA 94025, United States

At least two (and probably more) episodes of andesite to basaltic andesite magma recharge and differentiation led to the accumulation of the large ~ 45 to 50 km<sup>3</sup> of rhyodacitic magma beneath Mt. Mazama. These recharge events are recognized on the basis of Sr concentrations in plagioclase phenocrysts and matrix glasses in both rhyodacitic pumices and andesitic scoria. Strontium concentrations of plagioclase phenocrysts in rhyodacitic tephra erupted during earlier smaller volume ~ 2 km<sup>3</sup> Llaor Rocks 7015 ± 45 yr.B.P. (Bacon, 1983) and shortly preceding Cleetwood eruptions provide some temporal constraints (200-170 years) on the timing of these magma recharge episodes. An electron microprobe and FTIR study of glassy melt inclusions in rhyodacitic tephra from the climactic, Cleetwood and Llaor Rocks eruptions was initiated in order to observe the temporal variation in dissolved volatiles (H<sub>2</sub>O, CO<sub>2</sub>, Cl, S, F) concentrations in the accumulating rhyodacitic magma body. Dissolved volatiles concentrations and trace element data are used to evaluate the effectiveness of magma recharge as a potential eruption trigger for the climactic eruption.

Several samples from various stratigraphic levels of the climactic, Cleetwood and Llaor Rocks pumice fall sequences were selected for the melt inclusion study. Rhyodacitic melt inclusions in plagioclase and orthopyroxene in climactic tephra range from felsic dacite (68-69% SiO<sub>2</sub> anhydrous) to rhyolite (70-73% SiO<sub>2</sub> anhydrous). Total dissolved H<sub>2</sub>O concentrations determined by FTIR range from 4.3 wt.% to 6.0 wt.%. Dissolved CO<sub>2</sub> concentrations were below detection level (~ 20 ppm) in all climactic rhyodacitic inclusions. Chlorine concentrations range from 1720 ppm to 3930 ppm in less evolved inclusions. Dissolved sulfur concentrations range from 70 to 300 ppm with highest sulfur concentrations occurring in high Cl and H<sub>2</sub>O inclusions. Dissolved fluorine concentrations range from 200 ppm to 900 ppm but do not exhibit any obvious correlation with other volatiles. Cleetwood melt inclusions span the same composition range as observed in climactic samples (68-73% SiO<sub>2</sub>). Total dissolved H<sub>2</sub>O concentrations by FTIR range from 4.2 to 5.4 wt.%. Dissolved CO<sub>2</sub> concentrations were below detection in most inclusions although one inclusion with 4.22 wt.% H<sub>2</sub>O by FTIR has 60 ppm CO<sub>2</sub>. Chlorine concentrations are similar to those observed in climactic inclusions and range from 1700 to 3950 ppm. Sulfur concentrations in Cleetwood rhyodacitic to dacitic inclusions range up to 500 ppm with several inclusions in the 330 to 450 ppm range. These high sulfur inclusions generally occur in inclusions with > 5.00 wt.% H<sub>2</sub>O and > 2100 ppm Cl. Llaor Rock rhyodacitic inclusions exhibit similar H<sub>2</sub>O concentrations but typically have much lower dissolved sulfur concentrations in the range of 60 to 130 ppm, with Cl concentrations from 1600 to 1800 ppm. Strontium and barium trace element data indicate that high sulfur, chlorine and H<sub>2</sub>O inclusions in Cleetwood and climactic phenocrysts can be attributed to fractionation from high Sr and sulfur basaltic andesite parent liquid(s) which recharged the chamber 170 years (or less) before the climactic eruption.

## V21C-13 1150h

### Ore Metal-rich Fluids Degassed from a Fractionating Magma Chamber in the Eastern Manus Basin, Western Pacific: Evidence from Melt Inclusions and Vesicles

Kaihui Yang<sup>1</sup> (416-978-0833;  
kaihui@geology.utoronto.ca)

Steven D. Scott<sup>1</sup> (416-978-5424;  
chair@geology.utoronto.ca)

<sup>1</sup>Department of Geology, University of Toronto, 22 Russell Street, Toronto, Ont M5S 3B1, Canada

Magmatic fluids are found in vesicular volcanic rocks that host several hydrothermal fields in the eastern Manus backarc basin. Dredged samples of fresh lavas, of basalt to rhyolite composition, define a calc-alkalic trend consistent with fractionation of a common source. Their vesicularity decreases with Si, K, Ba and Zr, and increases with Ca, Mg, Fe and Sr of the bulk samples, suggesting that the degassing of volatiles was

linked to crystal fractionation of the magma. The felsic rocks have much lower vesicularities (<10%) than the mafic rocks (>30%), indicating that the fractionated felsic magma lost most of its vesicles before its eruption. High concentrations of H<sub>2</sub>O (0.9 to 2.5%) and Cl (up to 0.45%) observed in the mafic melt inclusions in phenocryst minerals of the basaltic andesite point to a volatile-rich magma. A separate fluid phase is present in the melt inclusions so the magma must have been saturated with volatiles in the magma chamber. The volatiles exsolved as an immiscible fluid with increasing crystal fractionation, and the composition of the degassed magmatic fluid changed with the evolving magma. The fluid is CO<sub>2</sub>-dominated during the degassing of weakly fractionated mafic magma and becomes a mixture of CO<sub>2</sub> and H<sub>2</sub>O as H<sub>2</sub>O is increasingly exsolved from the highly-fractionated felsic magma. The ore metals in the degassed fluid, as inferred from the compositions (by EPMA, SEM/EDS and TOF-SIMS) of metallic precipitates in the vesicles of melt inclusions and matrix glass, progressively change from Ni+Cu+Zn+Fe in basalt and basaltic andesite, to Cu+Zn+Fe in andesite, Cu+Fe in dacite, Fe in rhyodacite and Fe+Zn (+Pb?) in rhyolite. This trend provides evidence that fluids, released from a fractionating magma, could be an enriched source of metals for various types of ore deposits. In particular, the pre-eruptive degassing of magmatic fluids from felsic magmas could be responsible for the Fe, Cu, Zn and Pb metals in the sulfide chimneys at PACMANUS and Susu in the eastern Manus basin. By analogy, a magmatic fluid can provide a major source of ore metals for large or super large volcanogenic massive sulfides deposits in the geological record of ancient island arcs.

## V22A MCC: Hall C Tuesday 1330h

### Melt Inclusions: What Do They Tell Us? II Posters (joint with OS)

**Presiding:** N Shimizu, Woods Hole Oceanographic Institution; C Mandeville, American Museum of Natural History

## V22A-1212 1330h POSTER

### Nano-Diamonds in melt inclusions in ortho- and clinopyroxene from mantle xenoliths, Salt Lake Crater, Hawaii.

Richard Wirth<sup>1</sup> (49-331-288-1319;  
wirth@gfz-potsdam.de)

Alexander Rocholl<sup>2</sup> (49-89-2180-6514;  
rocholl@petrol.min.uni-muenchen.de)

<sup>1</sup>GeoForschungsZentrum Potsdam, Telegrafenberg Div.4.1, Potsdam D-14473, Germany

<sup>2</sup>Ludw. Max. Univ. Munchen Dept. Geo- und Umweltwissenschaften Zentrallabor Isotopengeochemie, Theresienstrasse 41/III, Munchen D-80333, Germany

We observed nanocrystalline diamonds in magmatic rocks from Hawaii (Salt Lake Crater). They occur in mantle xenoliths (Ga-pyroxenites) in melt inclusions in ortho- and clinopyroxene. The xenoliths are incorporated in the host lava and have been transported from the Earth's interior to the surface by volcanic eruptions. Consequently, such xenoliths allow an insight into the structure, the chemical composition and the P-T conditions of the Earth's mantle. Salt Lake Crater pyroxenites are interpreted as high-pressure basaltic cumulates trapped and adiabatically cooled within the Hawaiian lithosphere at 1000° - 1150°C and 1.6-2.5 GPa (50-80 km). The melt inclusions were investigated by using TEM and AEM.

Specimen preparation was performed by focused ion beam technique (FIB) at the GeoForschungsZentrum Potsdam (GFZ). Promising melt inclusions in pyroxene have been selected from thin sections. FIB technique uses oil-free vacuum to avoid contamination of the foil. The resulting TEM foil has the dimensions 20 μm x 10 μm x 100 nm. Coating of the TEM ready foil with carbon was not necessary.

Nanocrystalline diamonds are embedded in melt droplets, which are enclosed in pyroxene crystals. The melt inclusions with an average diameter of about 5 μm are always associated with a fluid phase or gas. The matrix of the melt inclusion consists of amorphous material (basaltic glass) containing very small inclusions of e.g. ZnS, Fe-Pd-S, Ag and Ir-rich minerals, native nanocrystalline iron and copper. Most of the diamonds occur in approximately rectangular shaped aggregates of polycrystalline diamonds, between 20 and 500 nm in size. The grain size of individual diamonds within each aggregate varies from 5 to 50 nm. The diamonds have been identified by X-ray analysis, electron diffraction and by EELS. The carbon K-edge in the EEL spectra allows to discriminate diamond, graphite and amorphous

Modeling of Alaskan Frozen Soil: **MY Lee**, A F Fossum, D R Bronowski

1330 h **T22B-1148** *POSTER* The Effect of Change in Scale on Water Content Estimates Derived From Ground Penetrating Radar Data: **S Moysey**, R J Knight

1330 h **T22B-1149** *INVITED POSTER* Pressure Effects on Seismically Observable Properties of Sands: **MA Zimmer**, M Prasad, G Mavko

1330 h **T22B-1150** *POSTER* Ultrasonic Monitoring of CO<sub>2</sub> Uptake and Release from Sand Packs\*: **DA Toffelmier**, W L DuFrane, B P Bonner, B E Viani, P A Berge

1330 h **T22B-1151** *POSTER* Laboratory Testing of Acoustic Tomography in Rock Samples Using Regularization of Incomplete Data: **C Li**, R L Nowack, L J Pyrak-Nolte

1330 h **T22B-1152** *POSTER* A Study of Soil Dynamic Behaviors Over Large Scale Strains During Unconsolidated-Undrained Triaxial Testing: **Z Lu**, C J Hickey, J M Sabatier

1330 h **T22B-1153** *POSTER* Viscous Creep in Dry Unconsolidated Gulf of Mexico Shale: **C Chang**, M D Zoback

1330 h **T22B-1154** *POSTER* Linear Viscoelastic Modeling of the Deformation of Unconsolidated Reservoir Sands: **PN Hagin**, M D Zoback

1330 h **T22B-1155** *POSTER* SH-Wave Seismic-Reflection Evidence for a Tectonic Origin of Anomalous Stress in Near-Surface Unlithified Sediment, Midcontinent, United States: **EW Woolery**, J A Schaefer, Z Wang

1330 h **T22B-1156** *POSTER* A Comparative Study of Hydrostatic Pressure and Stress Field Conditions in Sands: **S Vega**, M Prasad, G Mavko, A Nur

1330 h **T22B-1157** *POSTER* Nonlinear Wave propagation at sediment layers: **K Tsuda**, R J Archuleta, D R O'Connell, F L Bonilla

1330 h **T22B-1158** *INVITED POSTER* Using Size Scaled Porosity Models for the Electrical Properties of Partially Saturated Porous Rocks and Soils: **AL Endres**

1330 h **T22B-1159** *INVITED POSTER* Hysteresis in the Low Frequency Electrical Response of Unsaturated Unconsolidated Sediments: **CA Ulrich**, L D Slater

1330 h **T22B-1160** *POSTER* High-Resolution Velocity-Depth Functions From a BSR Field at the Yaquina Basin off Peru: J W Grobys, **CP Huebscher**, D Gajewski, J Bialas

1330 h **T22B-1161** *POSTER* Full Wave Form Inversion of High Frequency OBH-Data from the Yaquina Basin off Peru: G L Netzeband, T A Minshall, **CP Huebscher**, J Bialas

1330 h **T22B-1162** *POSTER* Frequency response of the pore pressure wells - from tidal to seismic frequency -: **T Yanagidani**, Y Kano, F Yamashita

**T22C MCC: 105 Tuesday 1330h**  
**Volatiles in Earth's Mantle II** (*joint with S, V, DI, MR*)

*Presiding:* **K Fischer**, Brown University; **Q Williams**, University of California, Santa Cruz

1330 h **T22C-01** *INVITED* Transportation of H<sub>2</sub>O in Subduction Zones as an Entrance of Water to the Mantle: **H Iwamori**

1345 h **T22C-02** *INVITED* Hydration of Subducted Slabs Beneath Arcs: Seismological Constraints: **GA Abers**

1400 h **T22C-03** Depth Distribution of The Subduction Zone Earthquakes and Devolatilization Phase Equilibria of Subducting Slab: **S Omori**, T Komabayashi, S Maruyama

1415 h **T22C-04** *INVITED* Dynamic Consequences of a Volatile-Rich Mantle Wedge: **MI Billen**, M Gurnis

1430 h **T22C-05** On Fabric Transitions: Is Wet Olivine Fabric Important in Earth's Upper Mantle?: **S Karato**

1445 h **T22C-06** The influence of water on the development of lattice preferred orientation in olivine aggregates: **E Kaminski**

**1500 h**

**BREAK**

1520 h **T22C-07** Incorporation of OH in olivine at high pressure: new experimental results: **JL Mosenfelder**, N I Deligne, P D Asimov, G R Rossman

1535 h **T22C-08** *INVITED* Water Storage in the Mantle and Effect of Water on Mantle Dynamics: **E Ohtani**, K Litasov

1550 h **T22C-09** Mantle Dynamics and Water Content of the Earth's Mantle Transition Zone: **GC Richard**, M Monnereau, J Ingrin

1605 h **T22C-10** *INVITED* Whole-Mantle Convection and the Transition-Zone Water Filter: **D Bercovici**, S Karato

1620 h **T22C-11** Kimberlites are Melts from Volatile-Rich Lower Mantle: New Geochemical and Pb-W Isotopic Evidence for Existence of Undegassed Deep Lower Mantle: **KD Collerson**, B S Kamber

1635 h **T22C-12** Temporal Evolution of Water in the Mantle: **JE Dixon**

**V22A MCC: Hall C Tuesday 1330h**  
**Melt Inclusions: What Do They Tell Us? II Posters** (*joint with OS*)

*Presiding:* **N Shimizu**, Woods Hole Oceanographic Institution; **C Mandeville**, American Museum of Natural History

1330 h **V22A-1212** *POSTER* Nano-Diamonds in melt inclusions in ortho- and clinopyroxene from mantle xenoliths, Salt Lake Crater, Hawaii.: **R Wirth**, A Rocholl

1330 h **V22A-1213** *POSTER* Cooling Rate and Isothermal Crystallization Effects on Melt Inclusion Formation in MORB High-An Feldspar and High-Fo Olivine: **EJ Kohut**, R L Nielsen

1330 h **V22A-1214** *POSTER* Ca-rich Plagioclase in Island Arc Tholeiite: Approaches from Hydrogen Melting Experiments and Melt Inclusion Study: **M Hamada**, T Fujii

1330 h **V22A-1215** *POSTER* High-Ca Melt Inclusions in Primitive Shoshonites: Magma-Wall Rock Interactions?: **RA Leslie**, L V Danyushevsky

1330 h **V22A-1216** *POSTER* Source of Detrital Chrome Rich spinels with melt inclusions from the Cretaceous greywackes of the eastern Tethyan Himalayas: hot spot volcanics, not ophiolites: **B Zhu**, W S Kidd, D B Rowley, J W Delano, B S Currie

1330 h **V22A-1217** *POSTER* Melt Inclusion Volatile Contents, Pressures of Crystallization for Hawaiian Picrites, and the Problem of Shrinkage Bubbles: P Cervantes, V Kamenetsky, **P Wallace**

1330 h **V22A-1218** *POSTER* Melt Inclusion from Volcan Colima and Popocatepetl: melt generation by combined fractionation and degassing: **ZD Atlas**, G Sen, M Finny, J E Dixon

1330 h **V22A-1219** *POSTER* Pre-eruptive Volatile Content of Miyakejima 2000 Eruption: **A Yasuda**

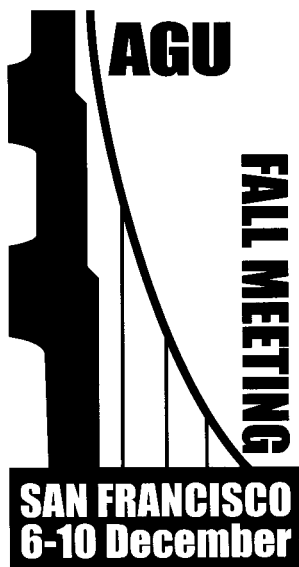
1330 h **V22A-1220** *POSTER* Glass Inclusion and Groundmass Glass Compositions in a Boninite: **RL Hickey-Vargas**

1330 h **V22A-1221** *POSTER* Melt Volatile Contents in Basalts From Lathrop Wells and Red Cone, Yucca Mountain Region (SW Nevada): Insights From Glass Inclusions: **JF Luhr**, T B Housh

1330 h **V22A-1222** *POSTER* Source Variations in Kamchatka Back-Arc Volcanism Inferred from a Mineral and Melt Inclusion Study of the South Chirpouk Monogenetic Center: **AO Volynets**, P Pletchov, T Churikova, M M Pevzner

# 2002

## Fall Meeting Program and Abstracts



This CD-ROM contains the program and abstracts of the 2002 Fall Meeting. The information is stored in both HTML and PDF formats as browsable tables and a searchable database. The CD-ROM is designed to run on Windows and Macintosh platforms.

### Software Requirements

A version 4.\* or later WWW browser (Netscape Navigator or MS Internet Explorer) with Java support is required to browse and search the abstracts. It is recommended to use the latest available browser release. To view, print or search the PDF files, the Adobe Acrobat Reader is required. To download, go to:  
<http://www.adobe.com/products/acrobat/readstep2.html>

### Installation Instructions

#### WINDOWS 9\*/ME/NT/2000/XP

The default page index.htm will be loaded automatically in the browser when the CD is inserted into the CD-ROM drive. No special installation of files on to the hard disk is required.

#### MACINTOSH

If your File Sharing Control Panel is configured to run the correct helper applications, the default page index.htm will be loaded automatically in the browser when the CD is inserted into the CD ROM drive. Otherwise, do the following:

1. Select "Run" to run MacStart script when prompted after inserting CD.
2. Choose Stuffit Expander to open Go.hqx (this starts Java console which will say "Waiting for client's request !!!").
3. Click the CD icon on the desktop and open index.htm in the browser.

Note for Macintosh OS X users: Refer to the README.txt file on the CD-ROM.

#### PDF-Search

As an alternative, a searchable index of the collection of session PDF files is included. See README.txt on the CD-ROM for more details.

#### Abstracts should be cited as

Eos Trans. AGU, 83 (47), Fall Meet. Suppl., Abstract XXXXX-XX, 2002  
©2002 American Geophysical Union

### Multi-Platform CD-ROM

(ISO 9660 + Joliet Extensions)

Windows 95/98/ME/NT/2000/XP  
Macintosh 8.\* or later